A peer-reviewed version of this preprint was published in PeerJ on 28 October 2014.

View the peer-reviewed version (peerj.com/articles/649), which is the preferred citable publication unless you specifically need to cite this preprint.

Walsh R. 2014. Are improper kinetic models hampering drug development? PeerJ 2:e649 https://doi.org/10.7717/peerj.649

Are improper kinetic models hampering drug development?

Reproducibility of biological data is a significant problem in research today. One potential contributor to this, which has received little attention, is the over complication of enzyme kinetic inhibition models. This over complication of inhibitory models stems from the common use of the inhibitory term $(1+[I]/K_i)$, an equilibrium binding term that does not distinguish between inhibitor binding and inhibitory effect. Since its initial appearance in the literature, around a century ago, the perceived mechanistic methods used in its production have spurred countless inhibitory equations. These equations are overly complex and are seldom compared to each other, which has destroyed their usefulness resulting in the proliferation and regulatory acceptance of simpler models such as ic50s for drug characterization. However, empirical analysis of inhibitory data recognizing the clear distinctions between inhibitor binding and inhibitory effect can produce simple logical inhibition models. In contrast to the common divergent practice of generating new inhibitory models for every inhibitory situation that presents itself, the empirical approach to inhibition modeling presented here, is broadly applicable allowing easy comparison and rational analysis of drug interactions. To demonstrate this, a simple kinetic model of DAPT, a compound which both activates and inhibits γ-secretase is examined using excel. The empirical kinetic method described here allows for a more in depth understanding of drug interactions and disease mechanism.

Are improper kinetic models hampering drug development?

Ryan Walsh*

Dept of Chemistry

Carleton University

Ottawa ON

rwalsh@connect.carleton.ca

PeerJ PrePrints | http://dx.doi.org/10.7287/peerj.preprints.521v1 | CC-BY 4.0 Open Access | rec: 2 Oct 2014, publ: 2 Oct 2014

Reproducibility of biological data is a significant problem in research today. One potential contributor to this, which has received little attention, is the over complication of enzyme kinetic inhibition models. This over complication of inhibitory models stems from the common use of the inhibitory term $(1+[I]/K_i)$, an equilibrium binding term that does not distinguish between inhibitor binding and inhibitory effect. Since its initial appearance in the literature, around a century ago, the perceived mechanistic methods used in its production have spurred countless inhibitory equations. These equations are overly complex and are seldom compared to each other, which has destroyed their usefulness resulting in the proliferation and regulatory acceptance of simpler models such as ic50s for drug characterization. However, empirical analysis of inhibitory data recognizing the clear distinctions between inhibitor binding and inhibitory effect can produce simple logical inhibition models. In contrast to the common divergent practice of generating new inhibitory models for every inhibitory situation that presents itself, the empirical approach to inhibition modeling presented here, is broadly applicable allowing easy comparison and rational analysis of drug interactions. To demonstrate this, a simple kinetic model of DAPT, a compound which both activates and inhibits γ-secretase is examined using excel. The empirical kinetic method described here allows for a more in depth understanding of drug interactions and disease mechanism.

The problem with classical inhibition models

Inhibitors bind to enzymes according to the same principles that govern ligand and receptor interactions. That is enzyme inhibitors are subject to the same mass action kinetic principles used to define the Hill-Langmuir equation and the Michaelis-Menten equation. However, the way enzyme inhibition equations are currently produced suggests that kinetically enzyme inhibitor interactions are as unique as the enzyme inhibitor system they are used to represent. This problem stems from the supposed mechanistic derivation of the principle inhibition equations, which resulted in an ambiguous inhibitory term that does not distinguish between the stoichiometric enzyme inhibitor binding interactions, defined by the inhibition constant (k_i) and the affect the inhibitor has on the enzyme.

The principal inhibition equations competitive, non-competitive and mixed non-competitive were derived from the reaction schemes depicted in Figure 1 (McElroy, 1947). As can be observed in the reaction scheme for competitive inhibition (Fig. 1a) the equation is based on the prevention of substrate binding to the enzyme when the inhibitor is present. This equation has been exclusively used to describe a blockage produced by the inhibitor binding to the active site of the enzyme. Alternatively the non-competitive inhibition equation (Fig. 1b) is derived from a reaction scheme where the inhibitor binds the enzyme substrate complex, and the mixed non-competitive inhibition equation (Fig. 1c) is used to describe inhibitors that are able to bind to the free enzyme or the enzyme substrate complex.

When the competitive inhibition equation is modeled an exclusive decrease in the substrate affinity (increase in K_1 value) is observed. In contrast the non-competitive equation produces an

exclusive decrease in the maximum reaction rate (V_1) and the mixed non-competitive inhibition equation describes inhibition where both substrate affinity and reaction rate are affected.

The flaws in the assumptions used to generate these inhibitory models are easy to identify and have resulted in the derivation of numerous additional equations to fill in the gaps. For example, changes in substrate affinity can result from mechanisms other than the inhibitor binding to the active site. Kinetic characterization of mutant enzymes or the comparisons of enzymes from different species has clearly demonstrated that substrate affinity directly relates to the spatial conformation of the active site. So competitive inhibition which is viewed as the predominant way in which inhibitors affect substrate affinity is not able to account for inhibitor interactions that alter the spatial conformation of the active site. An example of this false competitive inhibition is the inhibition of Kallikrein by benzamidine (Sousa et al., 2001). Inhibition of Kallikrein by benzamidine is known to result from benzamidine blocking the binding of peptide side chains but not the active site (Bernett et al., 2002). This results in a decrease in the peptidases substrate affinity but not the catalytic activity of Kallikrein, which can be conceptualized as the production of a new inhibitor derived surface which is less favorable for substrate binding (Walsh, Martin & Darvesh, 2011; Walsh, 2012).

The assumptions used to generate the non-competitive model only take into account complete catalytic inhibition. The schematic representation of this is usually depicted as an inhibitor binding to the enzyme in a location other than the active site (Fig. 1), inducing a change that prevents substrate hydrolysis. The main problem with this schematic representation is there is no way to distinguish kinetically between non-competitive and competitive inhibition using these models. In each case inhibitor binding would drive product formation to zero as inhibitors binding at the active site or in a peripheral location would prevent enzymatic catalysis.

Additionally the non-competitive inhibition model fails to consider situations where the inhibitor may only partially reduce the catalytic rate of the enzyme. Such effects can easily be rationalized by considering situations where the inhibitor binds and does not affect the substrate binding region but does alter the spatial conformation of the amino acids or cofactors involved in the catalytic activity, reducing the efficiency of the enzymatic activity.

The mixed non-competitive model, as a combination of the competitive and non-competitive models, describes inhibition that affects substrate affinity and the catalytic rate of the enzyme. However, based on the reaction schemes used to generate the competitive and non-competitive inhibition models both one to one enzyme inhibitor binding events are already accounted for (Fig. 1). To get around this problem the classical mechanistic theory suggests that mixed non-competitive inhibitor are able to bind to their target with two different inhibition constants (K_i and αK_i). This unusual theory excludes the possibility an inhibitor could affect both substrate affinity and catalytic activity in one enzyme inhibitor binding interaction.

One of the reasons that these models have endured for so long may be related to the false sense of security the equations for these models provide. The common form of the inhibitory term found in each equation suggests that the inhibition term $(1+[I]/K_i)$ is working in a similar way. This is actually completely incorrect as the inhibitory term in the competitive inhibition equation (Fig 1a) directly affects the substrate affinity (K_1) by multiplying into it, but the inhibitory term in the non-competitive inhibition equation (Fig 1b) inversely affects the maximum catalytic activity (V_1) by dividing into it. A rearrangement of the non-competitive inhibition equation demonstrates that the decrease in catalytic activity, it describes, is directly dependent on binding of the inhibitor through a term that is identical to the mass action terms used to describe, ligand

receptor interactions in the Hill-Langmuir equation and substrate enzyme interactions in the Michaelis-Menten equation, (equation 1).

$$v = V_1 \frac{[S]}{([S]+K_1)\left(1+\frac{[I]}{K_i}\right)} = \frac{[S]}{[S]+K_1} V_1 \times \left(1-\frac{[I]}{[I]+K_i}\right) = \frac{[S]}{[S]+K_1} \times \left(V_1 - V_1 \frac{[I]}{[I]+K_i}\right) \quad (1)$$

The implications of this are that the non-competitive inhibition equation is the only one of these three equations that is even somewhat correct. A similar rearrangement of the competitive inhibition inhibitory term demonstrates that the change in substrate affinity is not directly related to inhibitor binding, but rather results from the substrate affinity (K_1) being divided by the percent of the enzyme population which is not bound by the inhibitor. This inversion of the inhibitor mass binding term is very similar to the inversion of the Michaelis–Menten equation used in Lineweaver–Burk plots to provide a linear graphical method of determining enzyme kinetic constants (equation 2). This explains why changes in substrate affinity produced by the competitive inhibition equation can only be used to describe linear increases in the substrate affinity and why it is not useful for describing systems where the inhibitor produces a finite hyperbolic shift in the substrate affinity.

$$v = V_1 \frac{[S]}{[S]+K_1\left(1+\frac{[I]}{K_i}\right)} = V_1 \frac{[S]}{[S]+\frac{K_1}{\left(1-\frac{[I]}{[I]+K_i}\right)}} \quad (2)$$

This also suggests an explanation for the use of two binding constants in the mixed non-competitive inhibition equation as the inhibitory terms of the competitive and non-competitive equations are affecting the constants of the Michaelis-Menten equation in different ways (Walsh, 2012).

By tying inhibitory effects to mass action terms all three base inhibitory equations and the equations derived to explain situations they fail to cover, can be replaced with a simple empirical relationship (equation 3) (Walsh, Martin & Darvesh, 2011; Walsh, 2012).

$$v = \frac{[S]}{[S] + K_1 - (K_1 - K_{1i})\frac{[I]}{[I] + K_i}} V_1 - (V_1 - V_{1i})\frac{[I]}{[I] + K_i} \quad (3)$$

That is, virtually any inhibitor and enzyme interaction can be described as a shift in the catalytic activity that is directly dependent on the mass binding of the inhibitor molecules to the enzyme population being studied (Walsh, Martin & Darvesh, 2011). The change induced by the inhibitor can relate to substrate affinity ($K_1 \rightarrow K_{1i}$), maximum reaction velocity ($V_1 \rightarrow V_{1i}$) or both. This distinction between binding and effect provides an easy way of describing the vast spectrum of changes in enzymatic activity that can result from the influence of inhibitors or activators. The modularity produced by describing inhibition in this fashion also provides a base equation that can be expanded to explain more complex kinetic interactions.

Empirical modeling of complex inhibition kinetics

By recognizing that changes in enzyme kinetic parameters are linked to the mass binding of the inhibitor and enzyme populations, more complex situations can be rationalized and modeled in a simple logical fashion. For example one of the current targets for Alzheimer's disease treatment is γ-secretase which is involved in the processing of amyloid precursor protein into β-amyloid. One drug candidate DAPT (N-[N-(3,5-difluorophenacetyl)-L-alanyl]-S-phenylglycine t-butyl ester) has been described as having complex kinetic interactions with γ-secretase, in that at low amyloid precursor protein concentrations, low concentrations of DAPT have been observed to produce activation of γ-secretase catalytic activity but as DAPT concentrations are increased this turns into inhibition (Svedruzic, Popovic & Sendula-Jengic 2013). At higher concentrations of amyloid precursor protein DAPT only appears to inhibit the enzyme. This is further complicated by the substrate activation and inhibition of γ-secretase by amyloid precursor protein. However, these observations are all that is needed to produce a quick simple empirical model of this interaction. The fact that DAPT produces different effects at different amyloid precursor protein concentrations indicates that the enzyme can be considered to have multiple forms, at least one at low substrate concentration and one at higher concentrations. This is also supported by the apparent substrate activation of the enzyme at elevated substrate concentrations and subsequent substrate inhibition as the substrate concentration is further increased.

So to start with the substrate interactions can be modeled with an expansion of the Michaelis-Menten equation that accounts for change in the enzyme activity over increasing substrate concentrations (equation 4)(Walsh 2012).

$$v = V_1 \frac{[S]}{[S]+K_1} - V_1 \frac{[S]}{[S]+K_2} + V_2 \frac{[S]}{[S]+K_2} - V_2 \frac{[S]}{[S]+K_3} \quad (4)$$

At low substrate concentrations the substrate binding (K_1) can be described using a term that mimics the Michaelis-Menten equation. At higher substrate concentrations the binding of an additional substrate molecule (K_2) pushed the γ-secretase to an increased rate of substrate hydrolysis (V_2). At even higher substrate concentrations (K_3) the γ-secretase activity is inhibited by the substrate. Fitting this equation (*for examples see* Kemmer & Keller 2010) to the data however clearly indicates that the changes in catalytic activity induced by the substrate are too extreme to be described with hyperbolic curves of Michaelis-Menten like kinetics but are sigmoidal requiring Hill coefficients, (equation 5).

$$v = V_1 \frac{[S]}{[S]+K_1} - V_1 \frac{[S]^{H1}}{[S]^{H1}+K_2^{H1}} + V_2 \frac{[S]^{H1}}{[S]^{H1}+K_2^{H1}} - V_2 \frac{[S]^{H2}}{[S]^{H2}+K_3^{H2}} \quad (5)$$

With the enzyme described as different forms relating to substrate concentrations the effect of DAPT can be expressed quite easily. At high concentrations of amyloid precursor protein DAPT acts as a regular inhibitor of γ-secretase catalytic activity, where observed changes in catalytic activity directly relate to the fraction of the enzyme population bound by inhibitor as described by the mass action binding term. The effect on the substrate affinity and catalytic activity are both dependent on the same binding term and the inhibition mirrors the inhibition produced by

very high concentrations of substrate (equations 6, 7). This suggests that the inhibition by substrate at higher concentrations may relate to additional substrate interactions with γ-secretase rather than through substrate aggregation.

$$V_2 = V_2 - (V_2 - V_{2i})\frac{[I]^{Hxx}}{[I]^{Hxx} + K_{xx1}^{Hxx}} \quad (6)$$

$$K_2 = K_2 - (K_2 - K_{2i})\frac{[I]^{Hxx}}{[I]^{Hxx} + K_{xx1}^{Hxx}} \quad (7)$$

The effect on γ-secretase at low concentrations of amyloid precursor protein is only slightly more complex as it has to be described using two interactions between the enzyme and DAPT. In an expansion of the inhibitory term, (equations 8-9), almost identical to the expansion of the Michaelis-Menten equation above (equation 4), the stimulation at low concentrations of DAPT (V_{1is}, K_{1is}) and inhibition at high DAPT concentrations (V_{1ii}, K_{1ii}) are both described mathematically using mass action terms.

$$V_1 = V_1 - (V_1 - V_{1is})\frac{[I]^{Hx1}}{[I]^{Hx1} + K_{x1}^{Hx1}} + (V_1 - V_{1is})\frac{[I]^{Hx2}}{[I]^{Hx2} + K_{x2}^{Hx2}} - (V_1 - V_{1ii})\frac{[I]^{Hx2}}{[I]^{Hx2} + K_{x2}^{Hx2}} \quad (8)$$

$$K_1 = K_1 - \left(K_1 - K_{1is}\right)\frac{[I]^{Hx1}}{[I]^{Hx1} + K_{x1}^{Hx1}} + \left(K_1 - K_{1is}\right)\frac{[I]^{Hx2}}{[I]^{Hx2} + K_{x2}^{Hx2}} - \left(K_1 - K_{1ii}\right)\frac{[I]^{Hx2}}{[I]^{Hx2} + K_{x2}^{Hx2}} \quad (9)$$

So empirically without taking into account any information about the mechanism, a kinetic equation which describes two enzyme states produced by substrate concentration and three interactions between DAPT and γ-secretase can be produced (Fig. 2, Fig 3). This equation allows for the simple evaluation of DAPT as an inhibitor providing a straight forward way of interrupting the problems this compound may cause by increasing β-amyloid production at normal amyloid precursor protein concentrations (see supplementary information for constant definition). It also allows for facile hypothesis generation, such as, a dimmer of DAPT may be a practical way to eliminate the activation of γ-secretase produced by lower concentrations of DAPT.

A comparison of the work involved in producing the conventional mechanistic model versus the empirical approach described here also highlights the utility of this approach. Equation 5 and the expansions used to describe the interactions of DAPT were produced, analyzed, and fit to the data (see supplementary information for fitting) in a few hours using the solver feature of excel (Kemmer & Keller, 2010).

The classical mechanistic approach used to describe the same kinetic process involved the generation of a complex reaction schematic with 14 enzyme, substrate and inhibitor interactions (Svedruzic, Popovic & Sendula-Jengic 2013). This reaction scheme was used to define around 25 disassociation constants and 3 rate constants. The equation produced from this scheme had to be defined from a connection matrix which was then fed into Mathematica to produce a

simplified version that ultimately only had five kinetic constants, (equation 10). While equation 10 does contain fewer parameters than the 17 constants used in equation 5 to describe the effect of DAPT on γ-secretase, a comparison of the predicted values produced using equation 10 with the observed experimental data suggests that equation 10 does not fit the data very well (Fig. 2). Refitting the parameters of equation 10 only marginally improved the models ability to fit the observed data (Fig. 4).

$$v = \frac{V_1[S]\left(\frac{1}{1+\frac{[S]}{K_{si}}}\right)\left(\frac{1}{1+\frac{[I]}{K_{ii}}}\right) + V_2[S]\left(\frac{1}{1+\frac{[I]}{K_{ii}}}\right)\left(\frac{1}{1+\frac{[I]}{K_{ia}}}\right)}{[S]\left(\frac{1}{1+\frac{[S]}{K_{si}}}\right) + K_{0.5s}\left(\frac{1}{1+\frac{[I]}{K_{ii}}}\right)\left(\frac{1}{1+\frac{[I]}{K_{ia}}+\frac{[I]}{K_{si}}}\right)} \quad (10)$$

A boxplot of the residuals was used to examine the distribution of the residuals produced by the models (Fig. 5). While ideally plotting the calculated against the observed data should produce a correlation of 1 (Fig. 4) with a symmetric distribution of the residuals around zero, a clear negative asymmetric distribution of the residuals is associated with equation 10 (Fig. 5a). Refitting the kinetic parameters associated with equation 10 improved the correlation (Fig. 5b) and also improved the symmetric distribution of the residuals around zero (Fig 5b). Equation 5 however improves the correlation (Fig. 4c) as well as the symmetry and spread of the residual values (Fig 5c). However, as previously mentioned equation 10 only relies on five kinetic parameters while equation 5, when expanded to describe DAPT interactions, contains 17. Thus

the increase in kinetic parameters might be viewed as over fitting of the data, as models of greater complexity are able to produce improved fitting. To evaluate whether the improvement in fitting produced by equation 5 was a result of over fitting, equation 5 and 10 were compared using the bayesian information criterion (BIC) which penalizes increasing complexity in model selection (Burnham and Anderson, 2002; Faraway, 2004). Not surprisingly when the BIC was used to compare equation 10 with the results produced by refitting the kinetic constants of equation 10 (Fig 4 a & b), a significant improvement in the BIC was observer (published values BIC = 597, refit kinetic parameters BIC 515). Examination of the BIC value produced by equation 5 (BIC = 448) also suggested a significant improvement over the fit achieved with equation 10 even though the number of parameters had increased by 12.

The improper fit between equation 10 and the experimental data may relate to several factors, such as its lack of hill coefficients in the equation, even though individual hill coefficients were used in the initial description of the raw experimental data (Svedruzic, Popovic & Sendula-Jengic 2013). Additionally, equation 10 only models amyloid precursor protein over expression, which does not take into account normal cell line amyloid expression levels, i.e. the substrate concentration is defined as the amount of vector used to produce amyloid over expression. However, neither of these things can be easily evaluated due to the confusing form of the equation which includes terms that do not distinguish between binding and effect in addition to the lack of proper overlay of the kinetic model on the experimental data.

Concluding remarks

The information that can be gained through proper kinetic modeling is invaluable for the understanding of processes at the molecular level. The way mechanistic equations are currently developed obscures the relationships between binding constants and effect on the enzyme. This has led to the marginalization of the enzyme kinetic field in a decade where tremendous amounts of money are being funneled into the understanding of biology at the molecular level. While the improper use of kinetic models in drug development and the study of biological processes may not be the primary cause of the problems plaguing the biological sciences (Wadman, 2013) it is contributing to them. This is exemplified by the development of DAPT as a γ-secretase inhibitor, where Elan Pharmaceuticals simply characterized this compound with an ic50 (Dovey et al., 2001) resulting in more than a decade of research into a compound that holds very little promise of ever being useful in the treatment of Alzheimer's disease. This single example hints at the enormity of time, money and resources that have been lost resulting from the marginalization of enzyme kinetic in favor of simplified inhibition models or ic50s.

The failure of Alzheimer's disease drug candidates have been attributed to many factors such as the initiation of clinical trials without proper insight into therapeutic mechanisms, improper design of the studies and a lack of mechanistic understanding of the disease itself (Becker et al., 2014, Schneider et al., 2014). To address these issues Becker et al., 2014, have stated that the development of sound scientifically grounded mechanistic theories of disease progression needs to be a priority. While I agree with these ideas, the use of inappropriate kinetic models, which mask more complex molecular interactions, will continue to obscure both disease mechanism and potential therapeutic intervention.

List of Supplementary Materials

Data fitting in excel: secretase supplementary.xls

Definition of Equation 5 kinetic constants

References

Becker RE. Greig NH. Giacobini E. Schneider LS. Ferrucci L. 2014. A new roadmap for drug development for Alzheimer's disease. *Nat Rev Drug Discov.* 13:156.

Bernett MJ. Blaber SI. Scarisbrick IA. Dhanarajan P. Thompson SM. BlaberM. 2002. Crystal structure and biochemical characterization of human kallikrein 6 reveals that a trypsin-like kallikrein is expressed in the central nervous system. *The Journal of Biological Chemistry* 277:24562-24570.

Burnham KP. Anderson DR. 2002. Model selection and multimodel inference: a practical information-theoretic approach. Springer

Dovey HF. John V. Anderson JP. Chen LZ. de Saint Andrieu P. Fang LY. Freedman SB. Folmer B. Goldbach E. Holsztynska EJ. Hu KL. Johnson-Wood KL. Kennedy SL. Kholodenko D. Knops JE. Latimer LH. Lee M. Liao Z. Lieberburg IM. Motter RN. Mutter LC. Nietz J. Quinn KP. Sacchi KL. Seubert PA. Shopp GM. Thorsett ED. Tung JS. Wu J. Yang S. Yin CT. Schenk DB. May PC. Altstiel LD. Bender MH. Boggs LN. Britton TC. Clemens JC. Czilli DL. Dieckman-McGinty DK. Droste JJ. Fuson KS. Gitter BD. Hyslop PA. Johnstone EM. Li WY. Little SP. Mabry TE. Miller FD. Audia JE. 2001. Functional gamma-secretase inhibitors reduce beta-amyloid peptide levels in brain. *Journal of Neurochemistry* 76:173-181.

Faraway JJ. 2004. Linear Models with R. Chapman & Hall/CRC, Boca Raton, FL.

Kemmer G. Keller S. 2010. Nonlinear least-squares data fitting in Excel spreadsheets. *Nature Protocols* 5:267-281.

McElroy WD. 1947. The mechanism of inhibition of cellular activity by narcotics. *The Quarterly Review of Biology* 22:25-58.

Schneider LS. Mangialasche F. Andreasen N. Feldman H. Giacobini E. Jones R. Mantua V. Mecocci P. Pani L. Winblad B. Kivipelto M. 2014. Clinical trials and late-stage drug development for Alzheimer's disease: an appraisal from 1984 to 2014. *J Intern Med.* 275:251-83.

Sousa MO. Miranda TL. Costa EB. Bittar ER. Santoro MM. Figueiredo AF. 2001. Linear competitive inhibition of human tissue kallikrein by 4-aminobenzamidine and benzamidine and linear mixed inhibition by 4-nitroaniline and aniline. *Brazilian Journal Of Medical and Biological Research* 34:35-44.

Spitzer M. Wildenhain J. Rappsilber J. Tyers M. 2014. BoxPlotR: a web tool for generation of box plots. *Nature Methods* 11:121-122.

Svedruzic ZM. Popovic K. Sendula-Jengic V. (2013) Modulators of gamma-secretase activity can facilitate the toxic side-effects and pathogenesis of Alzheimer's disease. *PLoS One* 8:e50759.

Wadman M. 2013. NIH mulls rules for validating key results. *Nature* 500:14-16.

Walsh R. 2012. Alternative Perspectives of Enzyme Kinetic Modeling. In: Ekinci D. ed. Medicinal Chemistry and Drug Design. InTech. 357-372.

Walsh R. Martin E. Darvesh S. 2011. Limitations of conventional inhibitor classifications. *Integrative biology* 3:1197-1201.

Acknowledgements

I would like to thank Dr. Svedružić for kindly sharing the raw data from his study on DAPT and γ-secretase interactions.

Figure captions

Figure 1. Classic inhibition schemes. The A) Competitive B) Noncompetitive and C) Mixed-noncompetitive equations and the reaction schemes used to derive them. In the reaction schemes (E) equals enzyme, (S) equals substrate, (I) equals inhibitor and (P) equals product. In the equations (v) is equal to the velocity of the reaction, (V_1) is the maximum velocity commonly denoted as V_{max} (maximum velocity),(K_1) is the substrate binding constant commonly denoted as the K_m (Michaelis-Menten substrate affinity constant) and (K_i) is the inhibitor binding constant.

Figure 2. Modulation of γ-secretase by DAPT. Fitting of A) the mechanistic equation (Equation 10), B) Equation 10 refit and C) the proposed empirical equation (Equation 5) to the raw data for DAPT and γ-secretase interactions. Each Line represents a different level of β-amyloid expression (Svedruzic, Popovic & Sendula-Jengic 2013).

Figure 3. . Schematic of the interactions between γ–secretase, its substrate APP and DAPT. The catalytic hydrolysis of APP appears to be controlled by the number of molecules interacting with γ–secretase. Secondary binding of APP or DAPT increases the potential hydrolytic rate dramatically. However, interactions of a third APP or DAPT molecule shuts γ–secretase off suggesting the enzyme may become clogged or be highly regulated catalytically.

Figure 4. Global equation fitting to the experimental data. Correlation plots of experimentally observed reaction rates versus calculated values obtained using A) equation 10 with the reported kinetic constants (correlation r = 0.968), B) equation 10 with kinetic constants optimized in excel (r = 0.972) and C) equation 5 (r = 0.993).

Figure 5. Boxplot of the residuals associated with each data fitting. A) Residuals produced by equation 10 with the published values, B) residuals associated with the equation 10 after it was refit to the data and C) residuals associates with equation 5. Center lines show the medians; box limits indicate the 25th and 75th percentiles as determined by R software; whiskers extend 1.5 times the interquartile range from the 25th and 75th percentiles, outliers are represented by dots. Since equation 10 was not fit to background substrate concentrations, for A and B, n = 208, while for C (Equation 5) n = 230 sample points. This plot was generated using the web-tool BoxplotR (Spitzer et al., 2014).

Figure 1

A

$$v = V_1 \frac{[S]}{[S] + K_1\left(1 + \frac{[I]}{K_i}\right)}$$

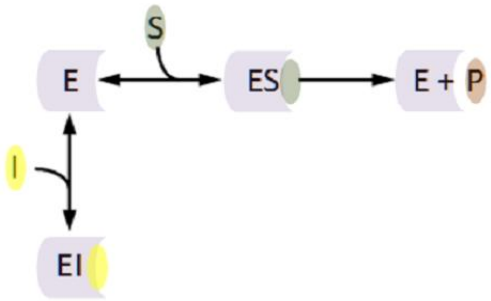

B

$$v = V_1 \frac{[S]}{([S] + K_1)\left(1 + \frac{[I]}{K_i}\right)}$$

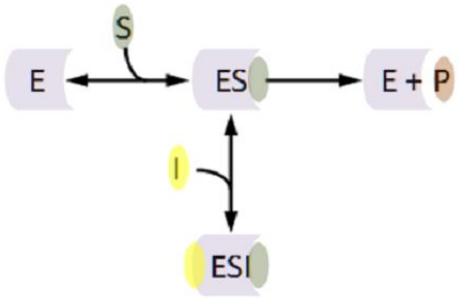

C

$$v = V_1 \frac{[S]}{[S]\left(1 + \frac{[I]}{\alpha K_i}\right) + K_1\left(1 + \frac{[I]}{K_i}\right)}$$

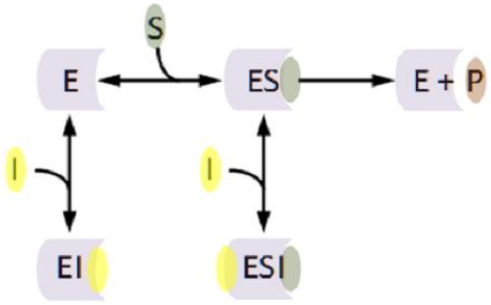

Figure 2

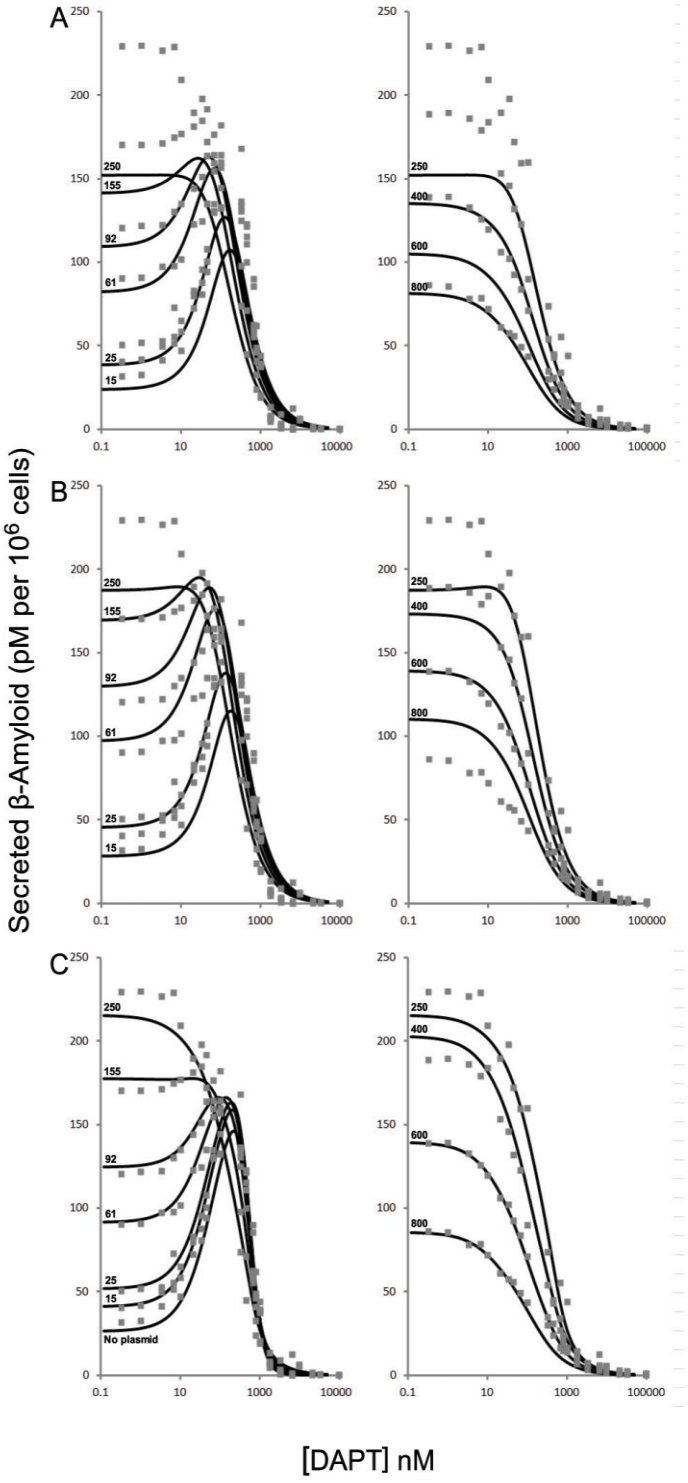

Figure 3

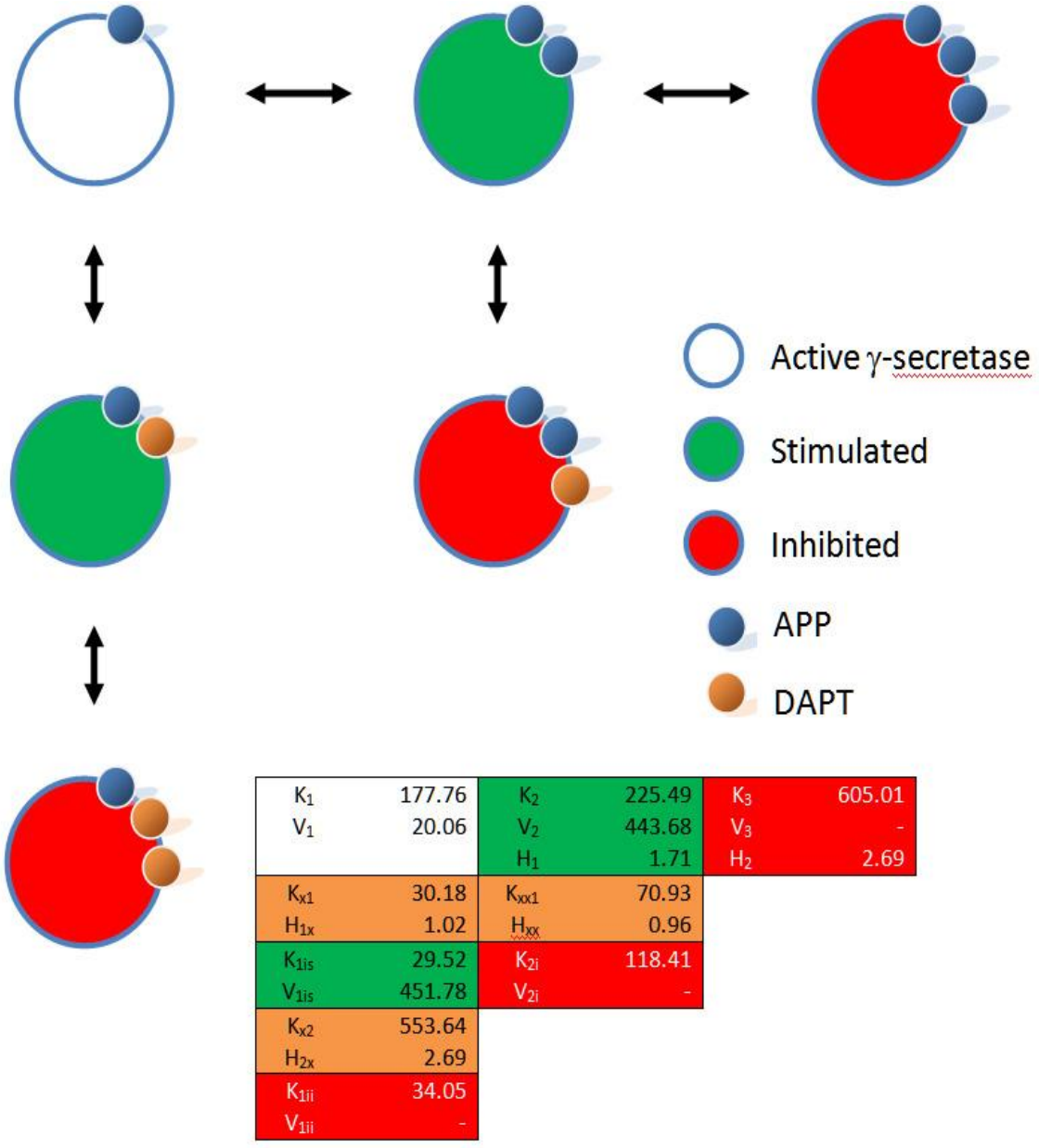

K_1	177.76	K_2	225.49	K_3	605.01
V_1	20.06	V_2	443.68	V_3	-
		H_1	1.71	H_2	2.69
K_{x1}	30.18	K_{xx1}	70.93		
H_{1x}	1.02	H_{xx}	0.96		
K_{1is}	29.52	K_{2i}	118.41		
V_{1is}	451.78	V_{2i}	-		
K_{x2}	553.64				
H_{2x}	2.69				
K_{1ii}	34.05				
V_{1ii}	-				

Figure 4

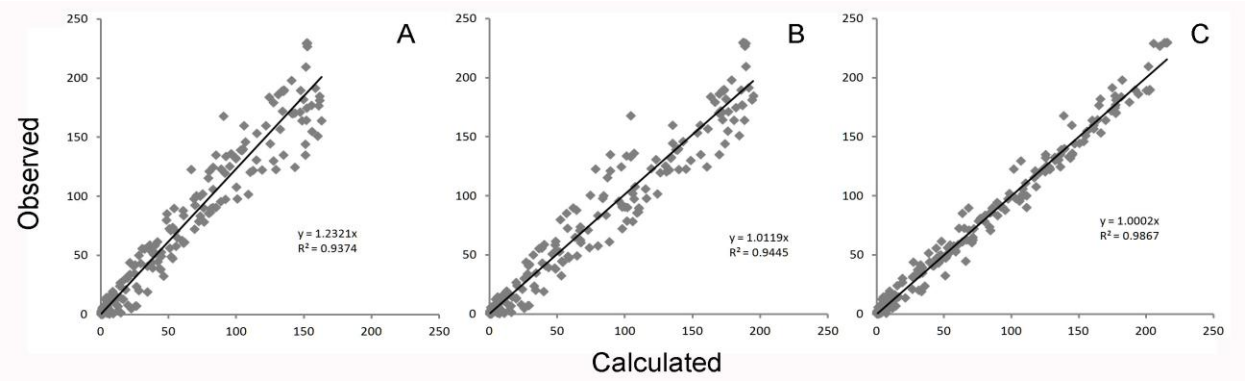

Figure 5